Electrochimica Acta, Vol. 33, No. 5, pp. 613–621, 1988.
Printed in Great Britain.

0013–4686/88 $3.00 + 0.00

THE INFLUENCE OF SLOW $Cu(OH)_2$ PHASE FORMATION ON THE ELECTROCHEMICAL BEHAVIOUR OF COPPER IN ALKALINE SOLUTIONS

J. GOMEZ BECERRA, R. C. SALVAREZZA and A. J. ARVIA

Instituto de Investigaciones Fisicoquímicas Teóricas y Aplicadas (INIFTA)*. Casilla de Correo 16, Sucursal 4, (1900) La Plata, Argentina

(*Received* 8 *April* 1987; *in revised form* 14 *September* 1987)

Abstract—Evidences of a slow $Cu(OH)_2$ phase formation with data resulting from potentiodynamic potentiostatic and rotating-ring-disc techniques were obtained during the anodization of copper in 0.1 M NaOH. According to the potential and time windows employed in the different runs, electrochemical results can be explained by admitting two limiting complex structures of the anodic layers namely Cu/Cu_2O (porous inner layer)/CuO (outer layer) and Cu/Cu_2O (porous inner layer)/$CuO/Cu(OH)_2$ (outer layer). The formation of the $Cu(OH)_2$ layer fits a progressive nucleation and 2-D growth under charge transfer control in the $-0.175 \leqslant E \leqslant -0.10$ V range and an instantaneous nucleation and 2-D growth mechanism under charge transfer control in the $-0.20 \leqslant E \leqslant -0.18$ V. A well-defined voltammetric peak multiplicity can be distinguished for the electrochemical of each complex anodic layer. These results furnish a reasonable explanation to discrepancies observed in the literature for the electroformation and electroreduction of anodic layers formed on copper in alkaline solutions.

INTRODUCTION

Passivating oxide layers formed on copper in alkaline media confer to the metal a good resistance against corrosion, and show interesting semiconducting properties for appropriate conditions of preparation. The electroformation of these layers involves as first oxidation stage the OH^- ion electroadsorption yielding a CuOH monolayer followed by the nucleation and growth of a tridimensional Cu_2O or CuOH layer[1–3]. The second oxidation stage is more complex involving the electroformation of a mixture of copper oxides and hydroxides in the +1 and +2 oxidation states of copper. Therefore, there is a basic agreement that the entire reaction implies the growth of the base Cu_2O layer, Cu dissolution as Cu(II) at pores of the Cu_2O layer, supersaturation followed by nucleation and growth of a $Cu(OH)_2$ film[4] and complete passivity caused by the electroformation of CuO filling the pores of the base film[5].

On the other hand, the kinetics and mechanism of electroreduction of these complex oxide layers is still a matter of discussion. Some authors consider that the mechanism of the reaction involves the electroreduction of Cu(II) oxide to Cu(I) oxide prior to the electroreduction of Cu(I) to Cu(O)[6], whereas others claim that the electroreduction of Cu(II) oxide to Cu(O) occurs at potentials more negative than those where the former reaction takes place[8]. Unfortunately, recent *in situ* optical data appears to be insufficient to clarify unambigously this mechanistic problem[9–11]. It seems likely that the discrepancies in the electroreduction reaction of copper oxide layers arise from the participation of slow uncontrolled processes in the overall reaction such as ageing of Cu(I) oxide and chemical reactions yielding new phase formation through a nucleation and growth mechanism. The relevance of this type of process during the passive oxide layer growth and correspondingly in the electroreduction reactions was recently suggested[9] although not convincingly demonstrated.

This paper provides new clear evidence about the role played by slow phase formation processes in the passivation of copper in alkaline solutions emerging from complemented potentiodynamic, potentiostatic and rotating-ring-disc electrode techniques.

EXPERIMENTAL

The working electrodes were made of polycrystalline (pc) copper rods (99.9%) axially embedded in Araldite holders to obtain exposed circular areas of 0.072 cm^2 apparent area. The electrode pretreatment consisted of a gradual polishing starting with fine grained emery paper followed with alumina paste (1 μm dia). Each polished specimen was successively rinsed in a.r. grade acetone, twice distilled water, and finally, dried in air at room temperature. The potential of the working electrode was measured against a saturated calomel electrode (*sce*) provided with a Luggin–Haber capillary tip. A platinum plate was used as counterelectrode. The electrodes were mounted in a conventional Pyrex glass cell. Measurements were made at 25°C ± 0.1°C in 0.1 M NaOH prepared from twice distilled water and NaOH (Merck p.a.), and purged with purified nitrogen for 3 h previous to each run. Singular triangular potential sweep (STPS) voltammograms between the cathodic ($E_{s,c}$) and the anodic ($E_{s,a}$) switching potentials at different sweep

* Facultad de Ciencias Exactas, Universidad Nacional de La Plata.

rates (v) were recorded as the apparent current density (j) *vs* potential (E) plots. The rotating-ring-disc technique (*rrde*) was used to detect soluble copper species either as Cu(I) or Cu(II) formed during the electrooxidation of copper. For this purpose a rotating gold ring (0.035 cm^2 apparent area) copper disc (0.125 cm^2 apparent area) electrode was used at rotation speeds (ω) in the $250 \leqslant \omega \leqslant 3000$ rpm range. Current transients at constant potential (E_s) were also recorded. In this case the following potential program was applied: firstly a cathodization at $E_c = -1.6$ V for 100 s to reduce any oxidized species, followed by a potential step to $E_{dl} = -0.80$ V (double layer region) for 20 s, and finally potential stepped to E_s ($-0.40 \leqslant E_s \leqslant 0.4$ V).

RESULTS

Voltammetric and rrde *data*

The positive potential going voltammetric scan of pc copper in 0.1 M NaOH run at 5×10^{-4} V s^{-1} between -1.4 and 0.3 V (Fig. 1) shows a rather asymmetric broad peak (A–I) at $E_{A-I} = -0.40$ V, a relatively large and sharp peak (A–II) at $E_{A-II} = -0.14$ V, and finally, a small hump (A–III) at the positive potential side. As $E_{s,a}$ is set increasingly positive a passive region can be observed. The reverse potential scan exhibits a small anodic current down to -0.2 V, then a small peak (C–III) at $E_{C-III} = -0.40$ V followed by a complex peak multiplicity which comprises a broad peak (C–I′) at $E_{C-I'} = -0.7$ V, a small one appearing as a hump (C–I″) at *ca* $E_{C-I''} = -0.78$ V, and a very sharp peak (C–II) at $E_{C-II} = -0.84$ V with a hump (C–I‴) at the negative potential side. Finally, at potentials more negative than -1.15 V, the HER current increases monotonously with the applied potential. Similar experiments made with values increased stepwise from -1.4 V to $E_{s,a}$ show that peak A–I is directly related to peaks C–I′, C–I″ and C–I‴, whereas peak A–II is mainly associated with peak C–II, and to a minor extent to peak C–I‴. Finally, there is a clear relation between peak A–III and peak C–III. Peak A–I was attributed to the electroformation of the Cu_2O/CuOH layer (1), and peaks A–II and A–III were assigned to the electroformation of Cu(II) hydroxide or oxide species (4).

To investigate the influence of v on the electroformation of copper oxide layers anodic runs were made at 0.001 V s^{-1} (Fig. 2) and 0.05 V s^{-1} (Fig. 2) between -1.5 and 0.65 V, but the complementary electroreduction scans were always made at $v = 0.05$ V s^{-1} between 0.65 and -1.70 V. For the anodic run made at 0.001 V s^{-1}, peak A–I appears as a broad contribution followed by well-defined peak A–II, although the latter looks rather asymmetric due to partial overlapping of peak A–III at the positive potential side. In this case, the corresponding electroreduction voltammogram presents peaks C–III, C–I′, C–II and C–I‴. On the other hand, for the anodic run at $v = 0.05$ V s^{-1}, the peak A–II appears not clearly defined whereas the peak A–III is no longer masked and it is now clearly visible. In addition, the corresponding electroreduction profile reveals a remarkable decrease of peaks C–II and C–I‴ and an increase of peak C–I′. The strong dependence of the electroreduction profiles on v resulting from these runs reveals the existence of time effect in the passive layer growth, that is the electroreduction profile depends on the history of the passivating layer. This effect, in principle, can explain why no simple voltammetric relationships are observed for current peaks involved in the electroformation of the Cu(II) passive oxide layers[12, 13].

The current–potential curves resulting from the rrde by potential scanning the copper disc at 0.01 V s^{-1}

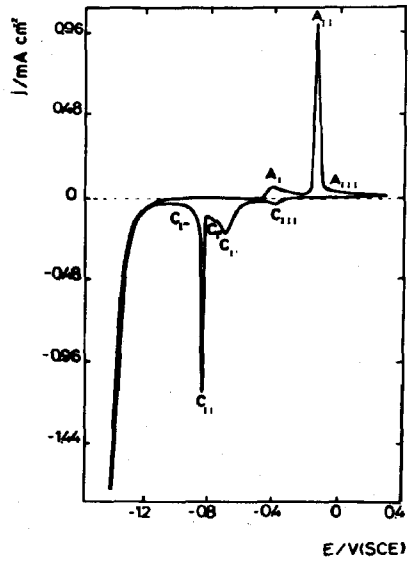

Fig. 1. STPS voltammogram of a copper electrode in 0.1 M NaOH at $v = 5 \times 10^{-4}$ V s^{-1} between $E_{s,c} = -1.4$ V and $E_{s,a} = 0.35$ V.

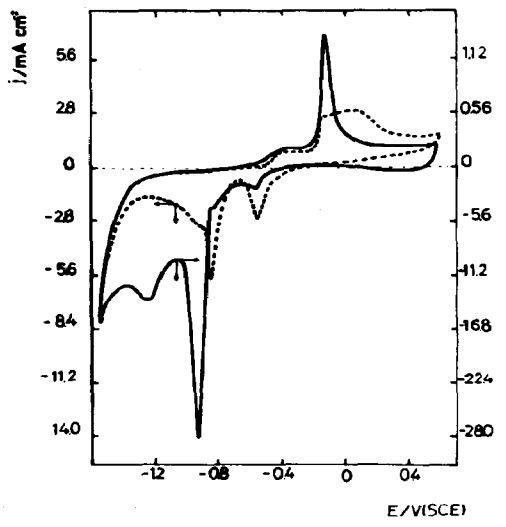

Fig. 2. STPS voltammogram of a copper electrode in 0.1 M NaOH between $E_{s,c} = -1.4$ V and $E_{s,a} = 0.35$ V at different v_a. (——) 1×10^{-3} V s^{-1}; (– – –) 0.05 V s^{-1}, $v_c = 0.05$ V s^{-1}.

between $E_{s,c} = -1.4$ V and $E_{s,a} = -0.10$ V, that is at the foot of peak *A*–II, show in the anodic scan a gradual current increase at potential more positive than E_{A-I} (Fig. 3a). In the -0.1 to -0.3 V range the returning scan exhibits an anodic current greater than that shown in the initial profile, followed by cathodic peaks *C*–I′ and *C*–I″ at more negative potential. When the potential at the ring (E_r') is held at -0.80 V in order to electroreduce both Cu(II) and Cu(I) soluble species to Cu(O), only a small amount of soluble species can be detected at potentials close to E_{A-I}, but a large amount of it can be detected at potentials more positive than E_{A-I} (Fig. 3b). Conversely, when E_r' is set at 0.0 V to electrooxidize soluble Cu(I) to Cu(II), measurable ring currents appear only at potentials close to E_{A-I} (Fig. 3c). Thus, the charge involved at potentials more positive than E_{A-I}, that is at the initial portion of peak *A*–II, corresponds directly to base copper electrodissolution as soluble Cu(II). Therefore, on the basis of the preceeding analysis, it is reasonable to assign the loop at the positive potential extreme of the voltammogram (Fig. 3) to an increase in the electrode area caused by corrosion of base copper. The increase in ω from 0 to 3000 rpm slightly enhances the current associated with the loop suggesting that the kinetics of the copper electrodissolution involves a certain mass transport of reactives to the bulk of the solution presumably occurring at pores from the base film (Fig. 4).

Current transients at constant potential and complementary voltammetric rrde *data*

Current transients resulting from constant potential steps (E_s) were recorded in the potential regions of peaks *A*–I, *A*–II and *A*–III by applying the following potential program: (i) electroreduction at $E_c = -1.60$ V for $t_c = 100$ s; (ii) potential stepped to $E_{dl} = -0.80$ V, that is to a potential just in the double layer region, for $t_{dl} = 20$ s; and (iii) potential stepped to E_s to record the corresponding current transient.

When E_s was held in the potential region of peak *A*–I, that is in the $-0.5 \leqslant E_s \leqslant -0.3$ V range, only decreasing current transients can be observed (Fig. 5a). Under these conditions an important contribution of soluble Cu(I) species can be determined through *rrde* during the current transient. To investigate the type of film formed during these current transients, anodic layers formed at $E_s = -0.30$ V for different t_s values were voltammetrically electroreduced at 0.05 V s^{-1}. In this case the layer was formed by applying the same potential program employed for current transients recording. When the layer formation time was $t_s = 10$ s, only peak *C*–I′ is observed in the electroreduction voltammogram (Fig. 6) together with a new contribution (*C*–I‴) overlapping the HER current. As t_s is increased, the potential of peak *C*–I′ moves in the negative direction, and simultaneously peak *C*–I‴ progressively emerges, and for longer t_s, peak *C*–I″

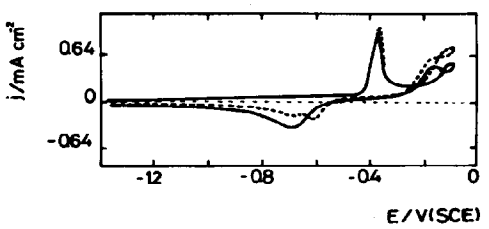

Fig. 4. STPS voltammogram of a copper rotating disc electrode at $v = 0.01$ V s^{-1} between $E_{s,c} = -1.4$ V and $E_{s,a} = 0.10$ V for $\omega = 0$ (——) and $\omega = 3000$ rpm (– – – –).

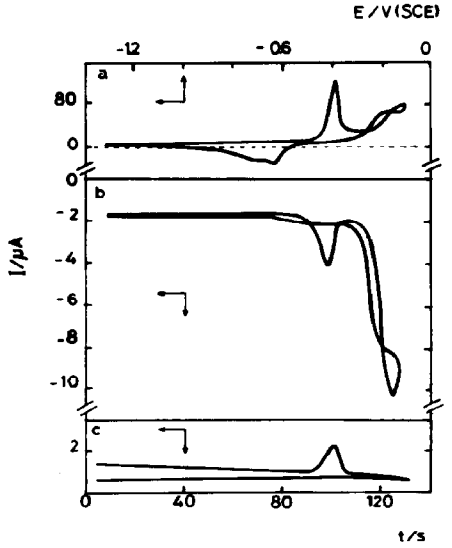

Fig. 3. (a) STPS voltammogram for a copper rotating disc electrode in 0.1 M NaOH at $v = 0.01$ V s^{-1} between $E_{s,c} = -1.4$ V and $E_{s,a} = -0.10$ V. (b) Ring current at $E_r' = -0.80$ V. (c) Ring current at $E_r' = 0.0$ V.

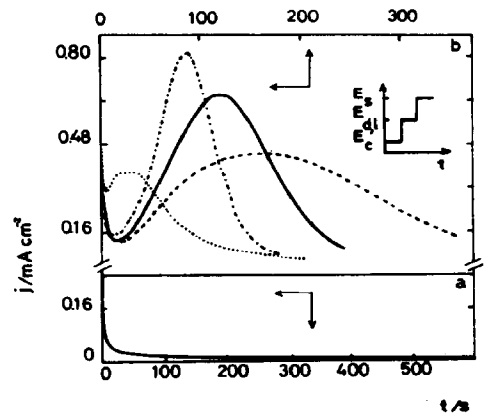

Fig. 5. (a) Current transients at constant potential ($E_s < -0.25$ V) for a copper electrode in 0.1 M NaOH. The potential program applied to the working electrode comprises a cathodization at $E_c = -1.60$ V for $t_c = 100$ s, an anodization at $E_{dl} = -0.80$ V for $t_{dl} = 20$ s, and finally potential stepped to t_s. (b) Idem as (a) for $E_s > -0.25$ V. (– – – –) -0.19 V, (——) -0.175 V, (–·–·) -0.15 V, (····) -0.05 V.

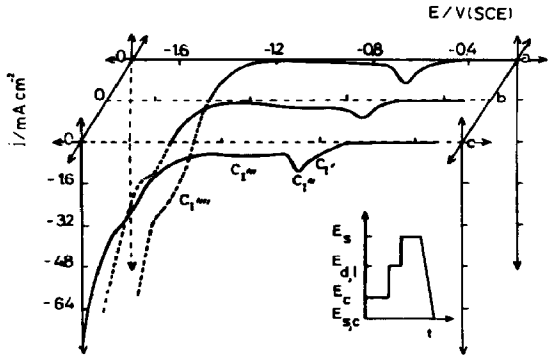

Fig. 6. Voltammograms at $v = 0.05$ V s^{-1} between $E_s = -0.30$ V and $E_{s,c} = -1.65$ V after anodization at E_s for different t_s values. Prior to the potential step at E_s the same potential program described for Fig. 5 was applied. (a) $t_s = 10$ s; (b) $t_s = 100$ s; (c) $t_s = 900$ s.

gradually develops at the negative potential side of peak C–I'. The charge density involved in peaks C–I', C–I'' and C–I''' apparently increases with t_s, whereas no marked change can be observed for that of peak C–I''''. These results reveal the importance of time dependent processes such as the ageing of Cu(I) oxide films in the voltammetric electroreduction profile as previously reported[1, 14].

When E_s is held in the potential range of peaks A–II and A–III the current initially exhibits a rapid decrease to a minimum value at the time t_i, and later increases to reach a maximum value (I_M) at the time t_M. Afterwards, it decreases to reach the small passivating current value at E_s. A representative set of these transients are shown in Fig. 5b.

Runs made in the $-0.25 \leqslant E_s \leqslant -0.15$ V range, show that the increase of E_s results in the increase of I_M, and correspondingly, the decrease in both t_M and t_i. For $E_s = -0.15$ V, the change in ω from 0 to 3000 rpm results in the charge increase of the transients recorded in the $0 < t_s < t_i$ range, while no remarkable changes are seen for $t_s > t_i$. The *rrde* data indicate that a large amount of soluble Cu(II) species is produced at $t_s < t_i$, although it progressively decreases for $t_s > t_i$.

On the other hand, runs made in the -0.15 V $\leqslant E_s \leqslant 0.0$ V range demonstrate that the increase of E_s results in the decrease of I_M, and correspondingly the charge involved in the transients. Otherwise, for $E_s > 0.0$ V only decreasing transients can be observed. Thus, in the $-0.25 \leqslant E_s \leqslant 0.0$ V range the shape of the transients is, in principle, consistent with the nucleation and growth of a Cu(II) layer which was assigned to hydrous $Cu(OH)_2$[4]. As the potential E_s is set closer to $E_{A\text{–III}}$ the nucleation and growth process becomes progressively hindered, and finally, it disappears ($E_s > 0.0$ V).

The characteristics of film formation at $E_s = -0.19$ V for different t_s values was also followed through the voltammetric electroreduction at 0.05 V s^{-1} (Fig. 7). Thus, when $t_s < t_i$ only peaks C–I', C–II'' and C–I''' appear in the voltammogram. Then, the decrease in the initial current should be associated with the electroformation of a complex base layer of Cu_2O and dissolution as detected by using the *rrde*. Otherwise, when $t_s > t_i$ peak C–II located at the negative side of C–I'' increases markedly. Accordingly, an increase in the contribution of C–I''' is also noticed at $t_s > t_i$. Clearly, peak C–II in this case results from the electroreduction of the $Cu(OH)_2$ layer which has been grown under a nucleation and growth mechanism.

Otherwise, when ω is changed from 0 to 3000 rpm

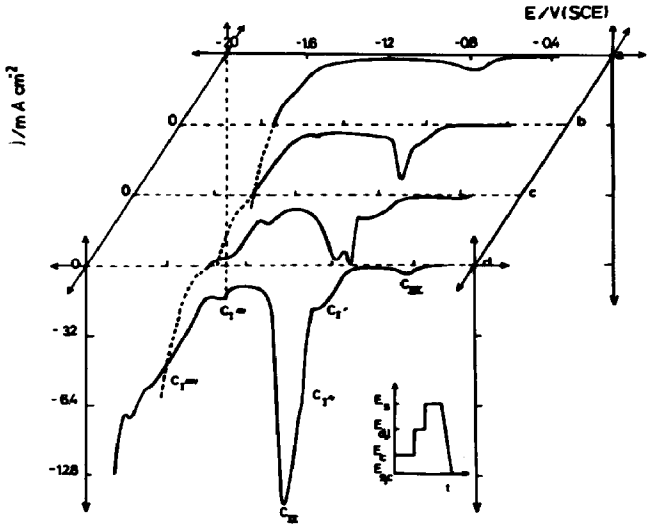

Fig. 7. Voltammograms at $v = 0.05$ V s^{-1} between $E_s = -0.19$ V and $E_{s,c} = -1.65$ V after anodization at E_s for different t_s values. Prior to the potential step at E_s the same potential program described in Fig. 5 was applied. (a) $t_s = 30$ s; (b) $t_s = 60$ s; (c) $t_s = 80$ s; (d) $t_s = 200$ s.

during t_s, that is during the layer formation, the charge of peak C–II remains unchanged, and peaks C–I, C–I″ and C–I‴ are also observed. This indicates that the complex Cu(I) oxide layer is still present on the copper surface. For large values of t_s peak C–III can be also detected.

Similar cathodic runs were made with anodic layers formed at different E_s values ($-0.25 \leqslant E_s \leqslant 0.2$ V) for $t_s = 300$ s (Fig. 8). In these cases the charge corresponding to peak C–II increases in the $-0.25 \leqslant E_s \leqslant -0.15$ V, whereas it decreases in the $-0.15 \leqslant E_s \leqslant 0.0$ V range. Finally, for $E_s > 0.0$ V peak C–II is no longer observed. Furthermore, the fact that peak C–I‴ decreases markedly as peak C–II decreases, suggests that peaks C–II and C–I‴ belong to conjugated processes. Conversely, as E_s is set increasingly positive the height of peak C–III increases but no marked changes in the heights of peaks C–I′ and C–I″ can be observed.

To obtain information about the stability of the hydrous $Cu(OH)_2$ layer at higher potentials, the anodic layer was formed by stepping the potential from the double layer region ($E_{dl} = -0.80$ V) to $E_s = -0.17$ V for $t_s = 100$ s, and later stepped to $E_s' = 0.20$ V for $t_s' = 200$ s. The corresponding electroreduction voltammograms exhibit peak C–II. The latter disappears when the step at $E_s = -0.17$ V is suppressed. Obviously, the hydrous $Cu(OH)_2$ layer which is stable at higher potentials, grows rather slowly within a narrow potential region ($-0.25 \leqslant E_s \leqslant -0.15$ V). At potentials more positive than -0.15 V the species formed in the potential range of peak A–III hinders progressively the nucleation and growth of the hydrous $Cu(OH)_2$ layer. Finally, if the applied potential is more positive than 0.0 V, the latter is no longer observed.

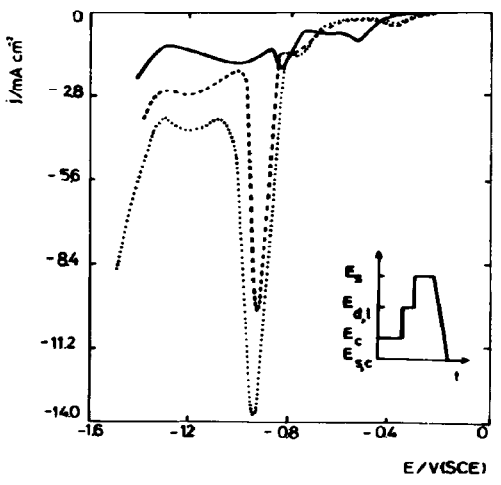

Fig. 8. Voltammograms at $v = 0.05$ V s^{-1} starting from different E_s after $t_s = 300$ s to $E_{s,c} = -1.65$ V. The potential program applied to the electrode before the voltammogram was described in Fig. 5. $E_s = (\cdots) -0.17$ V, (– – –) -0.10 V, (——) 0.2 V.

DISCUSSION

The complex electrochemical behaviour of copper in alkaline solutions involves the electroformation and electroreduction of different oxides or hydroxides layers accompanied by the formation of Cu(I) and Cu(II) soluble species according to potential and time windows used in the electrochemical measurements. To rationalize the discussion it is convenient to deal with the formation of the anodic layer within different potential ranges including the kinetic and some structural aspects of the reactions, and later, the electroreduction of the different anodic layers.

Anodic layers formed in the potential range of Cu/Cu(I) *redox system*

The first stage of the anodic formation comprises the build up of a $CuOH_{ad}$[1] monolayer and the electrodissolution of copper as Cu(I) species[2] followed by the growth of a Cu_2O or CuOH tridimensional layer (peak A–I). The threshold potential of peak A–I agrees with the reversible potential (E_r) for the reaction[15]:

$$Cu_2O + H_2O + 2e^- = 2Cu + 2OH^-; \qquad E_r(0.1\ M\ NaOH)/V(sce) = -0.538. \tag{1}$$

As previously reported[1] the electroreduction profile of the firstly formed anodic layer develops a peak multiplicity by increasing either the electroformation potential, E_s, or the electroformation time, t_s. The charge densities (q) of the different cathodic peaks ($q_{C\text{-}I'}$, $q_{C\text{-}I''}$, $q_{C\text{-}I'''}$) are practically independent of ω. These results suggest that various Cu(I) oxides or hydroxides layers attaining different electrochemical–chemical stabilities constitute the anodic layer formed on the copper surface[1]. Thus, the electroreduction of the most reactive components of the anodic should be related to peaks C–I′ and C–I‴′ which appear firstly in the electroreduction profile, whereas peaks C–I‴ and C–I″ should involve the electroreduction of most stable species as their contribution grows significantly according to t_s values. As an example, when E_s is set at -0.30 V, that is within the potential range of peak A–I, for 900 s, the subsequent electroreduction voltammogram involves mainly peaks C–I′, C–I″ and C–I‴, and the overall charge density (q_T) becomes close to 7 mC cm^{-2}, and time independent. In this case, the $q_{C\text{-}I'''}$ is relatively small and difficult to evaluate because of the overlapping of the HER. If one admits that the complex Cu(I) oxide layer approaches the Cu_2O stoichiometry, then, the layer thickness (h) can be roughly estimated from the value of q_T through the following equation:

$$h = \frac{M}{zF\rho} q_T, \tag{2}$$

where M and ρ are the Cu_2O molecular weight and density, respectively. For $M = 143$ g mole^{-1}, $z = 1$, $\rho = 6$ g cm^{-3} results in $h \simeq 173$ Å. Therefore, the following electrooxidation state of copper involves processes occurring on a surface already covered by a relatively thin anodic film.

Anodic layers in the potential range of Cu/Cu(II) *redox system*

The *rrde* data indicate that in $E_{A-I} \leqslant E_s \leqslant E_{A-II}$ potential range copper electrodissolves mainly as Cu(II) species. As in this potential range no marked changes in the electroreduction profiles of Cu(I) oxide layers can be observed, it can be concluded that the electrodissolution process likely involves the transport of Cu(II) soluble species at pores of the Cu_2O layer. Therefore, the ionic mass transport contribution to the entire reaction can explain the slight dependence of the anodic current on ω in this potential range, and correspondingly, the increase in the electrode area which reflects through a clear loop in the voltammogram. The reactions occurring in this potential range can be written as follows:

$$2CuO_2^{2-} + 3H_2O + 2e^- = Cu_2O + 6OH^-;$$
$$E_r(0.1\ M\ NaOH;\ 10^{-6}\ M\ CuO_2^{2-})/V\,(sce) = -0.34, \quad (3)$$

and

$$CuO_2^{2-} + 2H_2O + 2e^- = Cu + 4OH^-;$$
$$E_r\,(0.1\ M\ NaOH;\ 10^{-6}\ M\ CuO_2^{2-})/V\,(sce) = -0.44. \quad (4)$$

Reaction (3) should take place at the Cu(I) oxide layer while reaction (4) undergoes at the base of the pores. Reaction (3) implies the rebuilding of the Cu_2O layer in the subsequent reaction step.

When $E_s > -0.25$ V, the current transients resulting at constant E_s are consistent with the nucleation and growth of a Cu(II) film. Although peaked current transients cannot be taken as the unequivocal proof of a nucleation and growth mechanism[16], certain features concerning the microscopic nature of nucleation are manifested, such as the random scatter of the transient parameters (t_i, t_M) observed under the same experimental conditions (Fig. 9) and the direct observation of island type deposits[4]. Likewise, concerning the nature of products it should be noticed that for $E_s = -0.22$ V the formation of $Cu(OH)_2$ layer is feasible as E_s is more positive than E_r for the reactions:

$$Cu(OH)_2 + 2e^- = Cu_2O + H_2O + 2OH^-;$$
$$E_r\ (0.1\ M\ NaOH)/V\,(sce) = -0.264, \quad (5)$$

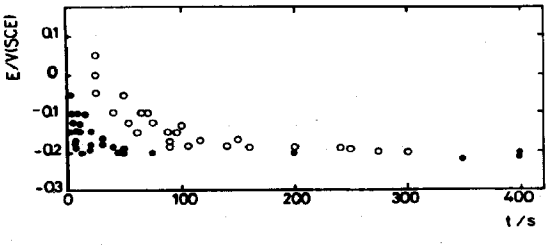

Fig. 9. t_i (●) and t_M (○) *vs* E_s for different current transients recorded in 0.1 M NaOH.

and

$$Cu(OH)_2 + 2e^- = Cu + 2OH^-;$$
$$E_r\ (0.1\ M\ NaOH)/V\,(sce) = -0.40. \quad (6)$$

This conclusion is confirmed by X-ray diffraction data which reveal the presence of a thick $Cu(OH)_2$ crystalline layer[4] for the layer formed in this potential range.

Nucleation and growth of hydrous $Cu(OH)_2$ *layer*

According to the present results when the potential is stepped from the double layer region to an E_s value comprised between -0.25 and -0.15 V, the nucleation and growth of the hydrous $Cu(OH)_2$ layer takes place. In the $-0.15 \leqslant E_s \leqslant 0.0$ V potential range the nucleation and growth processes become progressively hindered, and for $E_s > 0.0$ V they practically disappear.

According to previous work the nucleation of the hydrous $Cu(OH)_2$ layer is avoided when the reaction proceeds under rotation[4] as the required supersaturation condition for soluble Cu(II) species close to the electrode surface cannot be attained. This conclusion was derived from the increase in electrodissolution current with ω, then, the trend is observed for the peaked current transient to disappear and to turn into a shoulder. The present results confirm the fact that the amount of soluble Cu(II) species increases with ω, but they also show that the increasing Cu(II) electrodissolution masks the nucleation and growth processes which are all present. It also should be noticed that as derived from the electroreduction profile the charge of peak related to $Cu(OH)_2$ electroreduction (q_{C-II}) becomes independent of ω. This suggests that at least part of the anodic layer participates in a solid state nucleation process.

Further information about the kinetics of the nucleation and growth process can be derived from the analysis of the potentiostatic current transients. In this respect it was earlier reported[17] that the formation of CuO layer involves a simple nucleation and growth of conical centers model which accounted for current transients around the current maximum. Similarly, another model based on an instantaneous nucleation and 3-D growth under charge transfer control[18] was proposed for the $Cu(OH)_2$ electroformation at the initial portion of the current transients. Unfortunately these two models disregarded the fact that the current transients related to nucleation and growth of $Cu(OH)_2$ layer are actually obscured by the simultaneous relatively large current contributions due to Cu_2O layer formation and Cu electrodissolution.

The electroreduction voltammograms of anodic layers with a different history point out that Cu_2O electroformation at $E > -0.22$ V, mainly occurs when t_s is smaller than t_i. For such conditions the voltammogram only exhibits peaks *C*–I, whereas peak *C*–II which is directly related to the electroreduction of $Cu(OH)_2$ increases markedly only for $t_s > t_i$. On the other hand, as the electrodissolution current can be estimated from *rrde* experiments, the true nucleation and growth current transients for $Cu(OH)_2$ can be obtained from the overall current transients by taking data at $t_s > t_i$ and subtracting from them the background current related to the formation of Cu(II)

soluble species. The shape of current transients resulting from this calculation and the fact that at the maximum $j_M t_M/q_M \simeq 1$ suggest that a progressive nucleation and 2-D growth of $Cu(OH)_2$ under charge transfer control takes place in the $-0.175 \leqslant E_s \leqslant -0.10$ V range. The corresponding rate equation in terms of the instantaneous current density, $j(t)$, for this type of mechanism [19] is:

$$j(t) = \frac{zF\pi M}{\rho} hAk^2t^2 \exp\left(-\frac{\pi M^2 Ak^2 t^3}{3\rho^2}\right) = P_1 t^2 \exp(-P_2 t^3), \quad (7)$$

where $$P_1 = \frac{2F\pi M}{\rho} hAk^2;$$

and $$P_2 = \frac{\pi M^2 Ak^2}{3\rho^2}.$$

A is the nucleation rate and k is the growth rate constant. However, in the $-0.20 \leqslant E_s \leqslant -0.180$ V range, the current transients are more adequately described by an instantaneous nucleation and 2-D growth under charge transfer control. In this case[19]:

$$j = \frac{2zF\pi M}{\rho} hN_0k^2t \exp\left(-\frac{\pi M^2 N_0 k^2 t^2}{\rho^2}\right) = P'_1 t \exp(-P'_2 t^2), \quad (8)$$

where $$P'_1 = \frac{2zF\pi M}{\rho} hN_0k^2;$$

and $$P'_2 = \frac{\pi M^2 N_0 k^2}{\rho^2}.$$

Using equations (7) and (8), the current transients recorded in the $-0.20 \leqslant E_s \leqslant -0.10$ V range (Fig. 10) can be satisfactorily reproduced through the use of parameters assembled in Table 1. As E_s is set more positive, both P_1 and P_2 increase although the relative change of P_1 is smaller than that for P_2. From the P_1/P_2 ratio the overall charge involved in the transients, q_T, can be estimated according to:

$$q_T = \frac{1}{3}\frac{P_1}{P_2}, \quad (9)$$

from equation (7), or

$$q_T = \frac{P'_1}{2P_2},$$

from equation (8).

The change of q_T with E_s (Table 1) indicates that at potentials greater than -0.15 V the average film thickness decreases in agreement with the corresponding values of q_{C-II} as derived from electroreduction voltammograms. This fact which indicates an inhibition of $Cu(OH)_2$ electroformation correlates with the change in mechanism from an instantaneous to a progressive nucleation.

From the standpoint of the layer structure these results can be understood for an anodic layer made of different constituents where one of them involving Cu(II) species can largely prevent the nucleation and growth of $Cu(OH)_2$, the inhibiting species being presumably related to CuO formation. This is supported by the fact that the following reactions are thermodynamically possible in the potential region of peaks A-II/A-III:

$$2CuO + H_2O + 2e^- = Cu_2O + 2OH^-;$$
$$E_r(0.1\ M\ NaOH)/V\ (sce) = -0.353. \quad (10)$$

Therefore, according to the foregoing discussion one can conclude that the build-up of the $Cu(OH)_2$ layer competes with the CuO electroformation. Thus, at long times and lower potentials ($-0.22 \leqslant E_s \leqslant -0.15$ V) or at short times and $E_s > -0.15$ V a CuO film can be formed in agreement with previously reported data[20]. Otherwise, for $E_s > 0.0$ V, the electroformation of a CuO layer proceeds before $Cu(OH)_2$ nucleation and growth so that the latter process is no longer possible. Thus, for $E_s = 0.0$ V and $t_s = 300$ s, $q_{C-III} \cong 1.6$ mC cm^{-2}, so that for $M_{CuO} = 79.54$ g mole^{-1}, $\delta = 6.4$ g cm^{-3} and $z = 1$, equation (2) gives $h \cong 20$ Å. This means that a thin CuO layer is already able to suppress the growth of the $Cu(OH)_2$ layer. Consequently, when the potential is stepped or ramped from the double layer region upwards to $E_s > 0$ V at a high v, the $Cu(OH)_2$ layer can not be formed because of the large induction times this process involves. In this case the passive layer consists

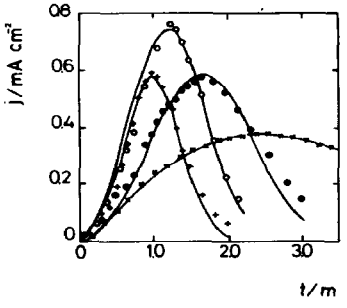

Fig. 10. Current transients at constant E_s for $t > t_i$ after subtracting the background current. (●) -0.175 V, (o) -0.150 V, (+) -0.125 V, (——) calculated with equation (7); (x) -0.190, (——) calculated with equation (8). Adjusting parameters are assembled in Table 1.

Table 1. Adjusting parameters used in the simulation of the current transients depicted in Fig. 10

Equation	E_s (V)	P_1 (mC cm^{-2})	P_2 (min^{-3})	q_T (mC cm^{-2})
(7)	−0.125	1.16	0.70	33.1
(7)	−0.150	0.96	0.36	53.3
(7)	−0.175	0.41	0.14	57.6
(8)	−0.190	0.257	0.088	88.2

mainly of an inner Cu_2O and an outer CuO layer[5]. However, if the potential program includes a previous step in the $-0.25 \leqslant E_s \leqslant 0.0$ V range, or a potential scan at a low v, the layer structure should approach a structure consisting of an inner Cu_2O, an intermediate CuO and an outer $Cu(OH)_2$ layer, the thickness of each layer depending on the operating conditions. The proposed structure for the passive film formed in this system under potentiostatic conditions at different E_s values has been schematically summarized in Fig. 11.

Application of the model to the voltammetric electroreduction profile

There is no agreement in the literature on the complex electroreduction profile of copper in alkaline media. It was reported that the electroreduction of Cu(II) oxide or hydroxide to Cu(I) species occurs before the electroreduction of Cu(I) oxide to Cu(O) takes place[5, 6]. Conversely, through galvanostatic measurements, some authors claim that the electroreduction of Cu(I) oxide to Cu(O) preceeds the electroreduction of Cu(II) oxide species[7]. *In situ* Raman spectroscopy of films formed on copper in 0.1 M NaOH indicates that peaks *C*–I′ and *C*–I″ are unambiguously assigned to the electroreduction of Cu_2O to Cu(O), whereas the nature of the peak at the negative side of peak *C*–I″ remains still obscure[8].

Recent spectroscopy data derived for a similar system support the idea that the small cathodic peak at the negative side of *C*–I″ can be assigned to the electroreduction of some $Cu(OH)_2$ placed at the top of the Cu_2O/CuO layers[10]. According to the present data the electroreduction profile and the optical data should be obviously strongly dependent on the experimental conditions for film formation. Therefore, the proposed model gives a reasonable account for the observed discrepancies. Thus, when the formation of $Cu(OH)_2$ is avoided, the cathodic curves show only peaks *C*–III and *C*–I. As E_r for reaction (10) is more positive than that of reaction (1), the electroreduction of the CuO film to Cu_2O occurs prior to the elec-

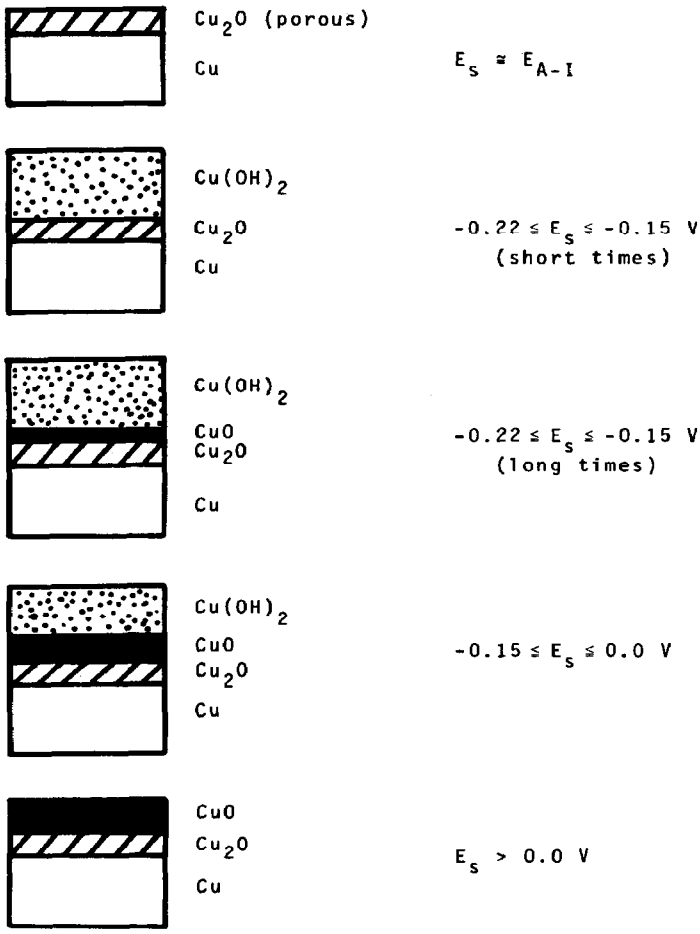

Fig. 11. Scheme showing the possible passive layer structures on copper at different E_s values compatible with the reaction model.

troreduction of Cu_2O to Cu(O). Conversely, when the $Cu(OH)_2$ layer is electroformed the cathodic profile becomes more complex. After anodization at $E_s = -0.19$ V for $t_s = 300$ s, q_{C-II} becomes of the order of 88 mC cm^{-2} and for $M = 97.56$, $\delta = 3.36$ g cm^{-3} and $z = 2$, equation (2) gives $h \simeq 1300$ Å. The electroreduction of this thick external layer can be probably assisted by the applied potential only when the inner CuO and Cu_2O layers have been reduced to Cu(O). Hence, the $Cu(OH)_2$ layer can be electroreduced to Cu_2O just in a narrow potential range associated with the sharp peak C–II which is followed by peak C–I''' corresponding to the electroreduction of Cu_2O to Cu(O). In this case a fine grained dark brown copper surface is formed when the overall electroreduction process is finished.

CONCLUSIONS

(1) The role of slow processes such as ageing of passive layers and nucleation and growth of a $Cu(OH)_2$ layer on the kinetics of electroformation and electroreduction of passive layer on copper in 0.1 M NaOH is established through the study of these reactions by combining potentiostatic current transients, voltammetric and *rrde* data.

(2) At $E_s > -0.25$ V the formation of $Cu(OH)_2$ layer competes with the electroformation of the CuO layer. The contribution of the former becomes increasingly relevant for relatively low applied overpotentials.

(3) According to the potential and time windows used in the different runs various passive layer structures on copper can be assigned, namely, such as: Cu_2O/CuO and Cu_2O/CuO/$Cu(OH)_2$. The amount of $Cu(OH)_2$ in the outer layer of the second structure apparently changes considerably by slightly modifying the experimental parameters.

(4) The voltammetric electroreduction profile involves firstly the electroreduction of the CuO layer to Cu_2O followed by the electroreduction of Cu_2O to Cu(O) over a relatively wide potential region (ΔE_{Cu_2O}). The electroreduction of the outer $Cu(OH)_2$ layer if present, takes place within a narrow potential range within the ΔE_{Cu_2O} region.

Acknowledgements—This research project is financially supported by the Universidad Nacional de La Plata, the Consejo Nacional de Investigaciones Cientificas y Técnicas and the Comisión de Investigaciones Cientificas de la Provincia de Buenos Aires. J.G.B. thanks to DAAD for his surplace fellowship.

REFERENCES

1. M. R. G. de Chialvo, S. L. Marchiano and A. J. Arvia, *J. appl. electrochem.* **14**, 165 (1984).
2. V. Ashworth and D. Fairhurst, *J. electrochem. Soc.* **124**, 506 (1977).
3. M. R. G. de Chialvo, J. O. Zerbino, S. L. Marchiano and A. J. Arvia, *J. appl. Electrochem.* **16**, 517 (1986).
4. D. W. Shoesmith, T. E. Rummery, D. Owen and W. Lee, *J. electrochem. Soc.* **123**, 790 (1976).
5. H. H. Strehblow and H. D. Speckmann, *Werkstoffe und Korrosion* **35**, 512 (1984).
6. R. L. Deutscher and R. Wood, *J. appl. Electrochem.* **16**, 413 (1986).
7. H. Pops and D. R. Hennessy, *J. Wire* **10**, 50 (1977).
8. J. S. Halliday, *Trans. Faraday Soc.* **50**, 171 (1954).
9. J. C. Hamilton, J. C. Farmer and R. J. Anderson, *J. electrochem. Soc.* **133**, 739 (1986).
10. Chon-Hong Pyun and Su Moon Park, *J. electrochem. Soc.* **133**, 2025 (1986).
11. J. L. Ord, D. J. DeSmet and Z. Q. Huang, *J. electrochem. Soc.* **134**, 831 (1987).
12. N. A. Hampson, J. B. Lee and K. I. Macdonald, *J. electroanal. Chem.* **32**, 165 (1971).
13. S. M. Abd El Haleem, *J. electroanal. Chem.* **117**, 309 (1981).
14. M. Maja and P. Spinelli, *Gazetta Chimica Italiana* **113**, 347 (1983).
15. U. Bertocci and D. Turner, In *Encyclopedia of Electrochemistry of the Elements*, (Edited by A. J. Bard) Vol. II, Marcel Dekker, New York (1974).
16. A. Sadkowski, *J. electroanal. Chem.* **208**, 69 (1986).
17. J. Ambrose, R. G. Barradas and D. W. Shoesmith, *J. electroanal. Chem.* **47**, 47 (1973).
18. F. Centellas, J. A. Garrido, J. Girones, E. Perez and J. Virgili, *Anal. Quimica* **80**, 193 (1984).
19. M. Fleischmann and H. R. Thirsk, In *Advances in Electrochemistry and Electrochemical Engineering*, (Edited by P. Delahay) Vol. 3, p. 123, Interscience Publishers, New York (1961).
20. D. W. Shoesmith, S. Sunder, M. G. Bailey, G. J. Wallace and F. W. Stanchell, *J. electroanal. Chem.* **143**, 153 (1983).